



Coronary vessel segmentation using multiresolution and multiscale deep learning



Zhengqiang Jiang^{a,*}, Chubin Ou^a, Yi Qian^{a,**}, Rajan Rehan^b, Andy Yong^{c,d}

^a Department of Biomedical Sciences, Macquarie University, NSW, 2109, Australia

^b Royal Prince Alfred Hospital, NSW, 2050, Australia

^c Department of Clinical Medicine, Faculty of Medicine and Health Sciences, Macquarie University, NSW, 2109, Australia

^d Department of Cardiology, Concord Repatriation General Hospital, NSW, 2139, Australia

A B S T R A C T

We present a coronary vessel segmentation method for X-Ray coronary angiography images using multiresolution and multiscale deep learning. Our segmentation method constructs a set of multiresolution images from an input image via bilinear interpolation, which can handle coronary vessels with uneven distribution of contrast. We incorporate Multiresolution and Multiscale Convolution Filtering into an U-Net Network, which can help to improve accuracy of segmentation results by dealing with various thickness of coronary vessels in different positions. We investigate two types of experiments of multiresolution strategy with U-Net and multiscale strategy with U-Net, respectively. Our method has been evaluated and compared both qualitatively with networks such as single U-Net, Attention U-Net, R2U-Net and R2AttU-Net, and quantitatively with 20 state-of-the-art visual segmentation methods using a benchmark X-Ray coronary angiography database. The experiments demonstrate that our segmentation method outperforms methods using each of these networks alone and these 20 methods significantly in terms of Dice Coefficient metric, which is considered as a major evaluation criteria of segmentation results.

1. Introduction

1.1. Motivation

Cardiovascular disease is one of major causes of human death in the world. Coronary vessel stenosis or plaque is one of most common and severe typical of cardiovascular disease. The early diagnosis of coronary vessel stenosis or plaque provides significant benefits for the treatment of cardiovascular disease. Different imaging techniques such as computed tomography angiography (CTA), Magnetic Resonance angiography (MRA), and X-Ray Coronary angiography (XRA) etc. have been used to diagnose stenosis or plaque of coronary vessels. Among all these techniques, XRA is considered as a golden standard for assessing the status of patient's coronary vessels [1]. For the XRA procedure, a catheter is inserted into coronary arteries and then contrast agent is injected through the catheter to darken coronary vessels in images, which can help cardiologists to efficiently find positions of stenosis and its grading.

However, cardiologists often face challenging problems while reading XRA images due to fatigue, patient's movement, heart beating, shape variation of vessels, noises, low contrast images, shadow and

catheter, and therefore sometimes provide unreliable diagnosing reports of XRA images. Fig. 1 shows two examples of XRA images with shadow or catheter. In addition, reading XRA images for cardiologists is very time-consuming. To reduce the burden from cardiologists, an automatic understanding of coronary vessel status is necessary. Prior to determine coronary vessel status, coronary vessel segmentation on XRA image using segmentation techniques is required. The aim of segmentation techniques is to extract coronary vessels in XRA images using computer vision and/or machine learning algorithms. The segmented vessels are used to compute image features such as vessel centrelines and widths at positions of vessels via skeleton models [4]. Such features can determine the locations of stenosis and topology structure of coronary vessels.

Numerous visual segmentation techniques have been proposed in the literature to segment coronary vessels. Several typical examples of traditional segmentation techniques consist of Watershed algorithm [40], Region-Growing algorithm [28] and active contour models [10]. Due to the recent promising results of visual object classification and recognition using deep learning models such as VGG [31], AlexNet [30], and GoogLeNet [33], more and more researchers have been applying deep learning models to image segmentation, particularly for semantic segmentation [25] which classifies each pixel belonging to foreground

* Corresponding author.

** Corresponding author.

E-mail addresses: zhengqiang.jiang@mq.edu.au (Z. Jiang), yi.qian@mq.edu.au (Y. Qian).

or background.

In this paper, we propose a multiresolution and multiscale based U-Net Network for coronary vessel segmentation. We firstly use a contrast limited adaptive histogram equalization algorithm to enhance input coronary images. Secondly, we compute a batch of multiresolution images at 4 scales for the enhanced images via bilinear interpolation. These multiresolution images are convoluted with a set of kernels under different scales and the output of convolutions in different scales are concatenated. We call this process as multiresolution and multiscale convolution filtering (MRCF). The output of MRCF is then integrated into an U-Net network [42] for vessel segmentation.

The research contributions of this paper are:

- A set of multiresolution images are designed to improve accuracy of the segmentation performance, especially when coronary vessels have uneven distribution of contrast.
- Our segmentation method incorporates Multiresolution and Multi-scale Convolution Filtering into an U-Net framework. This enables the system to deal with various thickness of coronary vessels in different positions.
- Without using a large number of XRA images as train data, our segmentation method outperforms methods using U-Net, Attention U-Net, R2U-Net and R2AttU-Net alone and 20 state-of-the-art visual segmentation methods significantly.

This paper is organized as follows. In the next section, we present the related work of our coronary vessel segmentation method. Section II describes the data set and our proposed coronary vessel segmentation method in detail, including contrast enhancement, multiresolution images, and multiresolution and multiscale based U-Net network. Experimental results will be shown in Section III. Section IV provides a discussion of our method. Finally, Section V gives conclusion and outlines future research direction.

1.2. Related work

Visual segmentation of coronary vessels in XRA images can be broadly classified

into 3 categories: Feature based [6–9,44], tracking based [11–13] and neural network based [2,3,16–19] methods.

Computing the Hessian matrix and its eigenvalues of an image [6,7] is a typical feature based method for segmenting coronary vessels. The Hessian matrix provides an effective way to represent features of tubular structure of vessels in images. This method is called as Hessian filter,

which has been widely used for vessel enhancement and segmentation. However, such a method tends to return uncontinuous segmentation results of vessels due to Hessian feature based on vessel geometry structure. Wan et al. [44] improved Hessian-based vessel segmentation by incorporating line-like features via a set of directional filters. Wang et al. [8] combined a region-growing algorithm with Hessian filtering for segmentation of coronary vessel images. The region-growing algorithm takes multiple pixels as seeds and merged each seed and its neighbourhoods into a same region using gray-scale histogram and k-means clustering method. However, their method often fails to segment vessels in complex situations such as noise and vessel stenosis due to an intensity based growing rule. To address this issue, a growing rule with vesselness and direction features was used for vessel segmentation [45]. Recently, Fazlali et al. [9] presented a coronary vessel segmentation method using a Simple Linear Iterative Clustering (SLIC) approach. The SLIC is one of superpixel algorithms, which searches for a pixel within a distance to the centre of a clustering and then assigns the pixel to the clustering.

Tracking based methods [11–13] often build deformable models for capturing the shape variation of coronary vessels through angiogram sequences. Nwogu et al. [11] presented a segmentation method of coronary vessels by tracking nonrigid centrelines of vessels. Similarly, Zhou et al. [13] demonstrated a segmentation method by tracking skeleton lines of vessels between angiogram frames. Zhang et al. [12] modelled coronary vessels as BSpline curves and tracked the landmark points in the curves. They treated the landmark points as nodes of a Directed Acyclic Graph (DAG) and location distance between landmarks as the edges of nodes. Tracking of coronary vessels between angiogram frames was performed by finding the minimal distance from the starting and ending nodes in the DAG.

Recently, neural network based methods have attracted more and more researchers due to promising results of vessel segmentation in medical images returned from the Convolutional Neural Network (CNN) architecture [14,15]. Fernando et al. [16] used Artificial Neural Networks (ANN) with a four-layer perceptron to segment coronary vessels. The ANN was trained with 100 angiograms and tested with 30 angiograms. Esfahani et al. [17] used a CNN architecture to conduct coronary vessel segmentation. They trained the CNN with 1040000 image patches which were generated by sliding a 33×33 window over 26 images with 512×512 sizes. To make the CNN architecture be more suitable for segmenting coronary vessels, Samuel et al. [3] incorporated vessel extraction operation which captures coronary vessel features into the convolution layers. Hao et al. [2] used 3D convolutional layers in CNN architecture to capture temporal-spatial features through coronary

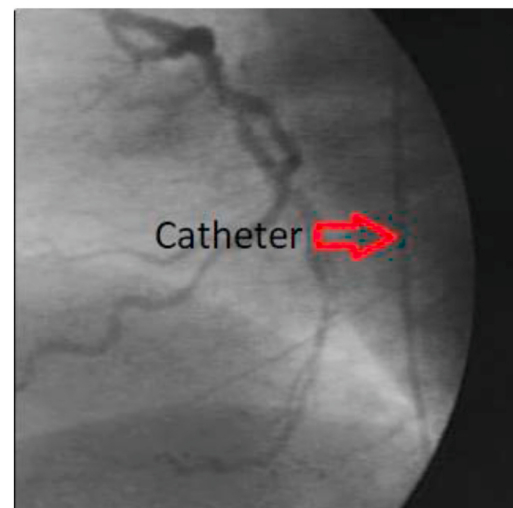
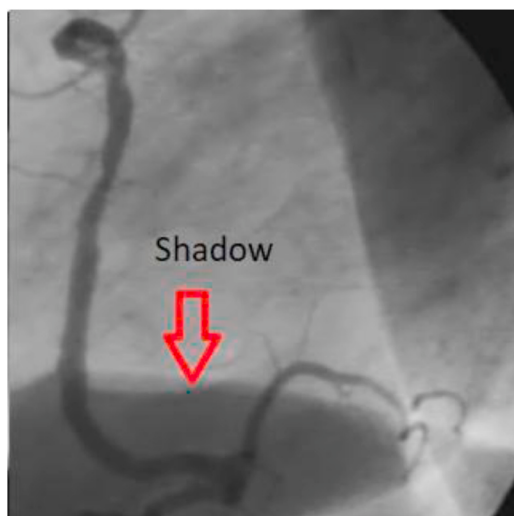


Fig. 1. Two examples of XRA images with shadow (the left) or catheter (the right).

sequential images. To get global context information, Zhu et al. [46] used a pyramid scene parsing network which concatenates vessel features generated by a CNN in different scales. Recently, Yang et al. [18] integrated an U-Net model into the CNN architecture for vessel segmentation. The U-Net model consists of two parts: convolutional encoder and deconvolution decoder. The convolutional encoder part reduces feature dimension of vessel images using downsampling while decoder part increases feature dimension to the size of input images using upsampling. Most recently, Jun et al. [19] extended the U-Net model to T-Net model for the segmentation of coronary vessels. The T-Net model consists of nested U-Net models in order to provide multiple concatenate layers between the encoder and decoder parts.

Segmentation performance can be improved by incorporating an inception model [5] into the CNN architecture. Our multiscale convolutions strategy reported in this paper shares similarities with the inception model, but also differs in some respects. The inception model uses convolution kernel scales with 1×1 , 3×3 , 5×5 only while we add scale 7×7 and combine a ReLU function for each scale. In addition, the input image features of our multiscale strategy were based on a set of multiresolution images, instead of the inception model using an original resolution image.

2. Materials & method

2.1. Materials

We used a database [16] consisting of 134 XRA images and the corresponding ground-truth images. Ground-truth images have labels of coronary blood vessels. Of these images, 94 images were used as training set, 10 images for validation set and 30 images for testing set. The size of each image is 320×320 pixels. Images in the training and testing set are selected from different patients.

2.2. Methods

The block diagram of our coronary vessel segmentation method, shown as 2 sub-diagrams, is illustrated in Fig. 2. Our proposed method incorporates MRCF as shown in Fig. 2 (b) into an U-Net network as shown in Fig. 2 (a).

1) Contrast Enhancement

XRA images often have low contrast between vessels and the background due to low dose usage of x-ray for minimizing the radiation exposure to operators. We use Contrast Limited Adaptive Histogram Equalization (CLAHE) [20] algorithm to enhance XRA images because it is fast and produces good contrast enhancement. The CLAHE algorithm divides an image into unoverlapped regions and conducts histogram equalization for each region.

Fig. 3 shows an example of XRA image and the contrast enhancement result from the CLAHE algorithm. From this figure we can see that the intensity difference of coronary vessel and background between the XRA image and enhanced one has been increased.

2) Multiresolution Images

The widths of coronary vessel in angiograms largely depend on the viewing distance of x-ray machine. Each patient also has various widths of coronary vessels. In Frangi et al.'s paper [48], four scales were evaluated on small and large vessels. We construct a series of multiresolution images from the original angiograms, as outlined below:

- The original angiograms are kept as one of multiresolution images;
- Using the bilinear interpolation, the size of the angiograms is changed by a number of scale factors to form the multiresolution images.

Fig. 4 shows an example of the original XRA angiogram and the constructed multiresolution images.

3) Multiresolution and Multiscales based U-Net Network

The U-Net consists of an encoder and a decoder part. The encoder uses two convolution operations with kernel size of 3×3 , followed by a ReLU activation function,

and a max-pooling operation with 2×2 filters and stride 2 for downsampling in each layer. The decoder applies upsampling with 2×2 transpose filters, 2 convolution operations with kernel size of 3×3 , and a ReLU activation function in each layer. The skip connections concatenate feature map after two 3×3 convolutions from the encoder part and the corresponding feature map after upsampling in the decoder part.

Due to uneven distribution of contrast through coronary vessels (see Fig. 5 (a)), segmentation results based on a single resolution image using an U-Net network may lead to fragments for continuous vessels. Fig. 5 (b) illustrates an example of segmentation results using an U-Net network with a single resolution image of Fig. 5 (a) as input. As shown in Fig. 5 (c), using multiresolution and multiscale based U-Net can provide accurate results of segmenting continuous coronary vessels.

In addition, an U-Net network conducts a single convolution operation with a filter size of 3×3 for a single scale image, which is not suitable for handling varying thickness of each vessel branch. Thus, segmentation results often can not accurately segment coronary branches in small or large widths.

To address these issues, we use multiresolution and multiscale based U-Net network to handle varying thickness of vessel branches. We incorporate MRCF for the encoder part of the U-Net network. Firstly, we construct a batch of multiresolution images described in section II-B.2 for each input image. These multiresolution images are then convoluted with different scales of convolution kernel (i.e. 1×1 convolutions, 3×3 convolutions, 5×5 convolutions and 7×7 convolutions) and followed by a ReLU activation function. Before the concatenation of multiresolution images, we map the images of different scales to the original resolution scale using bilinear interpolation. Finally, all convolution results over different convolution scales are concatenated and then fed to the next level of the encoder part of U-Net network. The multiresolution and multiscale based U-Net Network repeats 2 MRCF operations on each layer of encoder part to generate feature map, which is cropped to concatenate the corresponding feature map from the same layer of decoder part.

3. Results

Experiments were carried out on a PC with Intel Xeon Bronze 1.9 GHZ and Nvidia Quadro Rtx5000. The operating system is Windows 10 Pro. Our coronary vessel segmentation method was coded using Python and deep learning libraries including PyTorch, Numpy and OpenCV.

For contrast enhancement, the clipLimit was set to 12 and tileGrid-Size was set to (8, 8). We used 4 multiresolution scales (0.75, 1, 1.25, and 1.5) for the construction of multiresolution images for U-Net network. These 4 scales were set empirically. For our segmentation network, the number of epochs was set to 500; the learning rate was set to 0.005; batch size was set to 1. We use Adam optimization algorithm with beta1 = 0.9 and beta2 = 0.999 to train our segmentation network. The loss function were BCELoss and DiceLoss. The depth of U-Net was 5. The convolution stride was set to 1 and padding was set to 0.

To evaluate the performance of our segmentation method with state-of-the-art methods quantitatively, we have used 5 evaluation metrics, namely, Accuracy, Sensitivity, Specificity, Positive Predictive Value, and Dice Coefficient [49]. The 5 metrics were computed as follows:

$$\text{Accuracy} = \frac{TP + TN}{TP + FP + TN + FN} \quad (1)$$

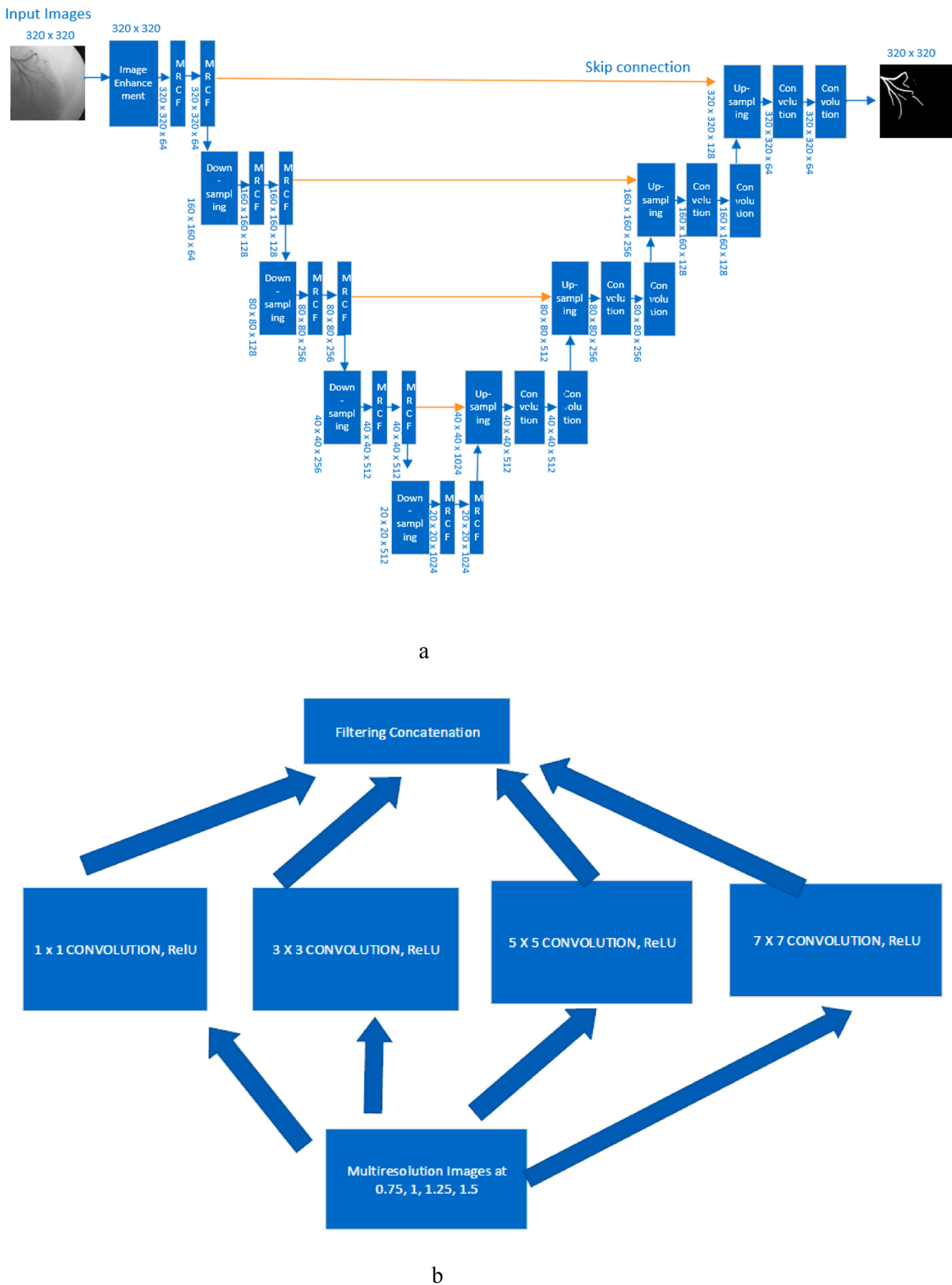


Fig. 2. A block diagram showing our coronary vessel segmentation on XRA images. (a) Multiresolution and Multiscale based U-Net Network. (b) MRCF.

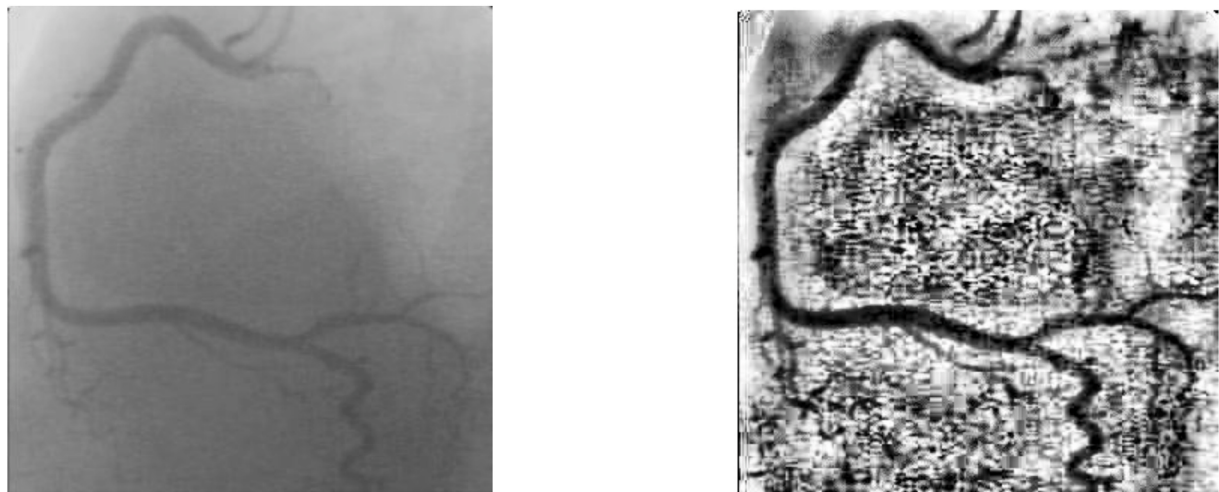


Fig. 3. An example XRA image and contrast enhancement result using the CLAHE algorithm.

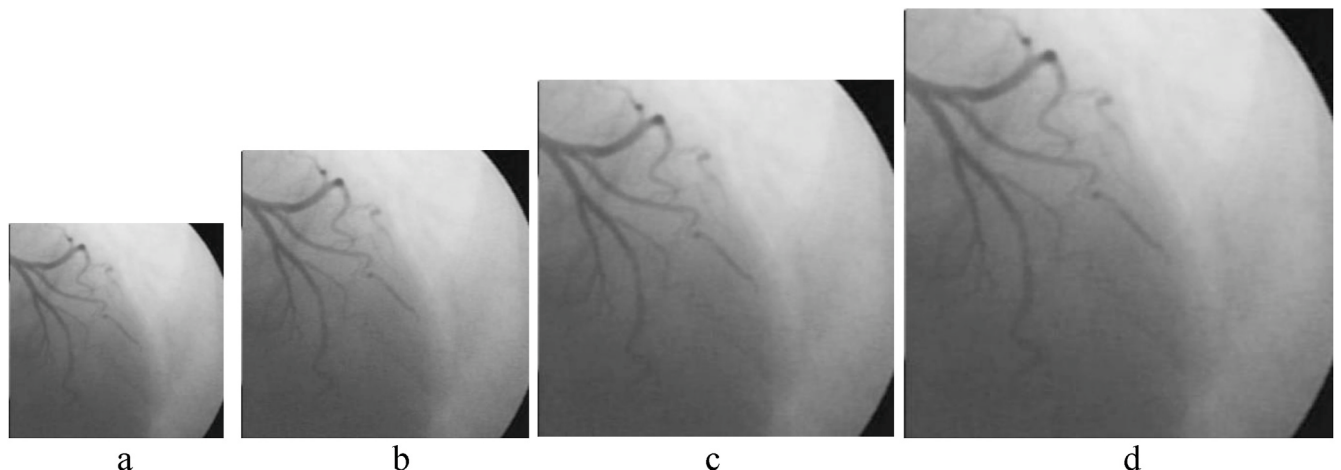


Fig. 4. The multiresolution images at scales 0.75 (a), 1.25 (c), and 1.5 (d) constructed from the original resolution (b) via bilinear interpolation.

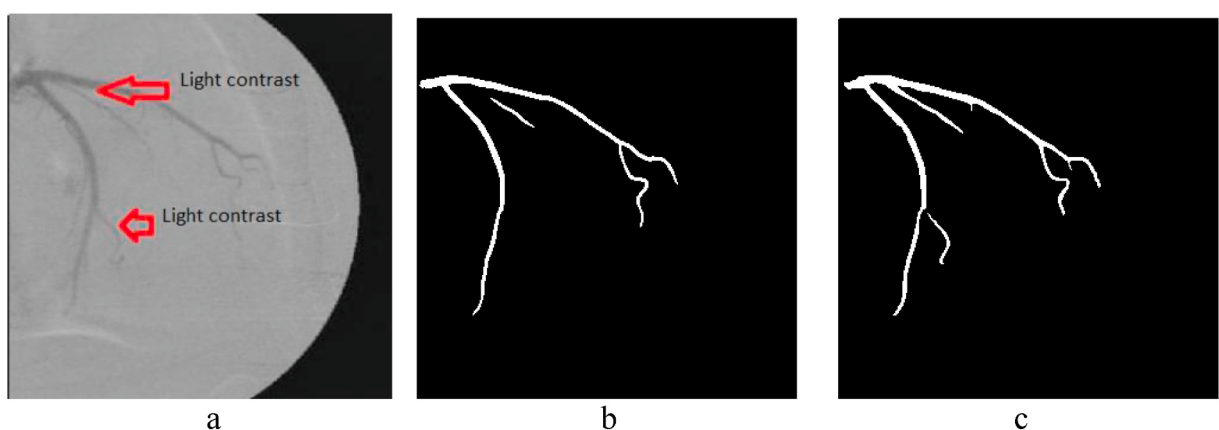


Fig. 5. An example of segmentation results on an image with uneven distribution of contrast (a) an original image (b) segmentation result on a single resolution of the input image (c) segmentation result on multiresolution of the input image.

$$\text{Sensitivity} = \frac{TP}{TP + FN} \quad (2)$$

$$\text{Positive Predictive Value} = \frac{TP}{FP + TP} \quad (4)$$

$$\text{Specificity} = \frac{TN}{FP + TN} \quad (3)$$

$$\text{Dice Coefficient} = \frac{2 \times |GT \cap SR|}{|GT \cup SR|} \quad (5)$$

where True Positive (TF) was defined as the number of correct foreground pixels; False Positive (FP) was defined as the number of incorrect foreground pixels; True Negative (TN) was defined as the number of correct background pixels; and False Negative (FN) was defined as the

number of incorrect background pixels, GT was defined as the ground truth, and SR was defined as the segmentation result. The 5 metrics are in the range [0, 1]. We set the threshold value of separating the foreground to background pixels to be 0.5. The value is determined empir-

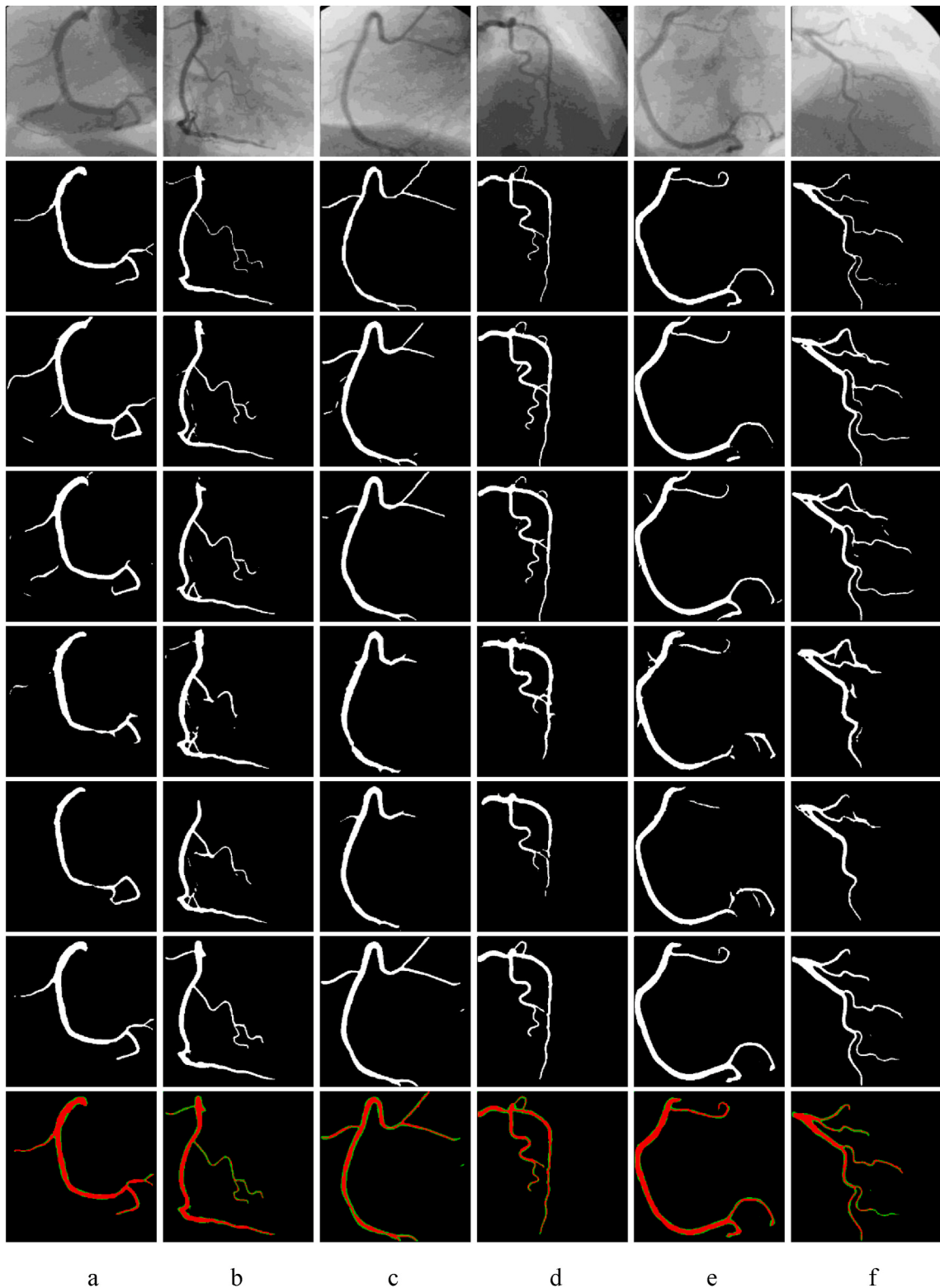


Fig. 6. The testing angiograms. Row 1: the original angiograms. Row 2: the ground truth of the angiograms. Row 3: The results of single U-Net method. Row 4: The results of Attention U-Net method. Row 5: The results of R2U-Net method. Row 6: The results of R2AttU-Net method Row 7: The results of our segmentation method. Row 8: The overlap between the results (in green) of our segmentation method and the corresponding ground truth (in red). (For interpretation of the references to colour in this figure legend, the reader is referred to the Web version of this article.)

ically. From these equations, we can see that a larger value of each metric indicates more robust of the method.

3.1. Qualitative evaluation

To illustrate the effectiveness of our coronary vessel segmentation method, we also conducted experiments that segment coronary vessels using single U-Net network, Attention U-Net [34], Recurrent Residual Convolutional Neural Network based on U-Net (R2U-Net) [26] and Recurrent Residual and Attention U-Net (R2AttU-Net) [27]. The single U-Net network shares all the same parameters with our multiresolution and multiscale based U-Net network, except for taking original resolution of angiograms as network inputs and the 3×3 size of convolution kernel alone.

Fig. 6 shows some examples of the segmentation results on the angiograms using single U-Net network, Attention U-Net, R2U-Net, R2AttU-Net and our method. From this figure we can see that single U-Net network, Attention U-Net, R2U-Net, R2AttU-Net tend to segment a continuous vessel into fragments (see the third row, fourth row, fifth row, sixth row of **Fig. 6**). One of possible reason is that the distribution of contrast along the coronary vessels is uneven. As shown in the seventh row of this figure, our segmentation method can segment the continuous vessels without segments. In addition, our segmentation method can accurately extract small and/or large sizes of vessels. The overlap between the results of our method and the corresponding ground truth is shown in the eighth row of this figure.

3.2. K-fold cross validation

We have conducted a K-Fold cross validation [36] to evaluate our coronary vessel segmentation methods. Parameter K was set to 6 in our experiments. Each fold has 22 angiograms and each angiogram is assigned to one fold only. Each fold has a chance of being test data and the remaining folds being the train data. **Table 1** shows the quantitative evaluation using the K-Fold cross validation. From this table, we can see that our segmentation method gave similar values of Accuracy, Sensitivity, Specificity, Positive Predictive Value, and dice Coefficient for K-Fold cross validation. Therefore, our method can be general for an independent angiogram dataset.

3.3. Quantitative evaluation

We also conducted two types of experiments: multiscale strategy + U-Net and multiresolution strategy + U-Net. The multiscale strategy + U-Net integrated scales 1×1 , 3×3 , 5×5 and 7×7 into the convolution operation of U-Net model, instead of 3×3 convolution only. The multiresolution strategy + U-Net uses a set of multiresolution images constructed from an original image as input for the U-Net model. **Table 2** shows the quantitative results of these two strategies. It is clear that the multiresolution strategy + U-Net gave the better result with the higher

Table 1
The results of K-Fold cross validation of our method ($k = 6$).

	Accuracy	Sensitivity	Specificity	Positive Predictive Value	Dice Coefficient
Fold 1	0.9773	0.7984	0.9891	0.8155	0.7968
Fold 2	0.9739	0.7947	0.9853	0.8105	0.7894
Fold 3	0.9757	0.7960	0.9861	0.8128	0.7902
Fold 4	0.9763	0.7969	0.9875	0.8132	0.7901
Fold 5	0.9778	0.7984	0.9887	0.8155	0.7912
Fold 6	0.9747	0.7953	0.9852	0.8124	0.7898

Dice Coefficient (0.7752 in the Table) whereas the multiscale strategy + U-Net had the lower Dice Coefficient (0.7661 in the Table). Compared with the Dice Coefficient of method using Single U-net (in the **Table 3**), multiscale strategy + U-Net gave the highest Dice Coefficient of 0.7752, followed by Dice Coefficient of 0.7661 for the multiscale strategy + U-Net and single U-Net gave the lowest Dice Coefficient of 0.7571. This indicates the effectiveness of multiresolution strategy and multiscale strategy with U-Net, respectively.

Table 3 demonstrates the comparison of segmentation results between our method and other 20 methods including single U-Net network, Attention U-Net, R2U-Net and R2AttU-Net. From this table we can see that our method provides the highest Accuracy value (0.9765), the highest Specificity value (0.9885), the highest Positive Predictive Value (0.8137), and the highest Dice Coefficient (0.7905). Compared to the single U-Net network method, the performance of our method is significantly improved from 0.7165 to 0.7978 and 0.7571 to 0.7905 in terms of Specificity and Dice Coefficient, respectively. Although the Sensitivity value of our segmentation method are lower than other 13 methods except single U-Net, Attention U-Net, R2U-Net, R2AttU-Net, VSSC Net [3], SVS-net [2] and Fernando et al.'s method [16], the Positive Predictive Value and Dice Coefficient of our method are significantly higher than other 20 methods.

Fig. 7 shows the results of our method with different values of batch size. From this figure we can see that our method with the value of batch size as 4 provides the best performance with highest dice coefficient.

3.4. Execution time

Table 4 shows the comparison of average execution time per image between our method and other different U-Net based methods including single U-Net network, Attention U-Net, R2U-Net and R2AttU-Net. From the table it is evident that there was no significant increase in execution time when changing from single U-Net network (0.38 s) to our method (0.39 s).

4. Discussion

Although our method is used to the segmentation of coronary vessels in XRA images, it is also suitable for the segmentation of retinal blood vessels in Digital Retinal Images (DRI). Since our method takes greyscale images as training and testing data, segmenting retinal blood vessels using our method needs to convert DRI as colour images to greyscale images firstly. Other segmentation processes for retinal vessels are same as those of our method for coronary vessels. Due to the unavailability of coronary vessel disease information such as the position of stenosis and plaque in the public database, the performance of our method regarding coronary vessel pathology was not reported in this stage of the paper.

Since the CLAHE algorithm redistributes the histogram bins with the corresponding counts over a user-defined threshold to all the bins evenly, such an algorithm can prevent the enhancement of noise. However, the Frangi Filter [48] conducts image enhancement by computing a Hessian matrix with the second partial derivative of an image, which is sensitive to noise. For the unsharp masking technique [47], noise is often enhanced by the convolution operation between an image and a sharpen filter.

5. Conclusion

We have presented a coronary vessel segmentation method that integrates multiresolution and multiscale convolution filtering into an U-Net network for XRA images. Our segmentation method constructs a set of multiresolution images, which are convoluted with a set of kernels in different scales. It can therefore deal with coronary vessels with uneven distribution of contrast and various branch thickness in different positions. We have evaluated our segmentation method against 20 other competitive segmentation techniques on XRA images from a benchmark

Table 2

The results of multiscale strategy + U-Net and multiresolution strategy + U-Net.

	Accuracy	Sensitivity	Specificity	Positive Predictive Value	Dice Coefficient
Multiscale strategy + U-Net	0.9730	0.7693	0.9871	0.7960	0.7661
Multiresolution strategy + U-Net	0.9729	0.7890	0.9865	0.7897	0.7752

Table 3

Comparison of segmentation results of ours method and other 20 methods on the testing data of 30 angiograms.

	Accuracy	Sensitivity	Specificity	Positive Predictive Value	Dice Coefficient
Our method	0.9765	0.7978	0.9885	0.8137	0.7905
VSSC Net [3]	0.9749	0.7634	0.9857	0.7568	0.7738
SVS-net [2]	0.9736	0.7429	0.9843	0.8075	0.7693
Single U-Net [42]	0.9758	0.7165	0.9815	0.8129	0.7571
Attention U-Net [34]	0.9712	0.7378	0.9874	0.7901	0.7476
R2U-Net [26]	0.9719	0.5046	0.9852	0.6624	0.6116
R2AttU-Net [27]	0.9687	0.6018	0.9876	0.7037	0.6580
Fernando et al. [16]	0.9698	0.6363	0.9880	0.7434	0.6857
Otsu [21]	0.9173	0.9472	0.9157	0.3806	0.5430
Ridler and Clavard [22]	0.9164	0.9478	0.9147	0.3779	0.5403
Niblack [23]	0.9146	0.9370	0.9134	0.3717	0.5322
Moment-preserving [51]	0.9081	0.9589	0.9053	0.3565	0.5197
RATS [24]	0.8989	0.9646	0.8953	0.3350	0.4973
Vessel repair [29]	0.8902	0.9664	0.8860	0.3168	0.4772
Sauvola [32]	0.8884	0.9639	0.8843	0.3130	0.4726
Entropy maximization [35]	0.8853	0.9744	0.8804	0.3082	0.4683
Background unification [50]	0.8757	0.9721	0.8704	0.2909	0.4478
Degree-based [37]	0.8581	0.9840	0.8512	0.2656	0.4183
White [38]	0.8574	0.9682	0.8514	0.2627	0.4132
Histogram concavity [39]	0.8442	0.9871	0.8363	0.2480	0.3965
Local entropy [41]	0.8247	0.9900	0.8156	0.2270	0.3693

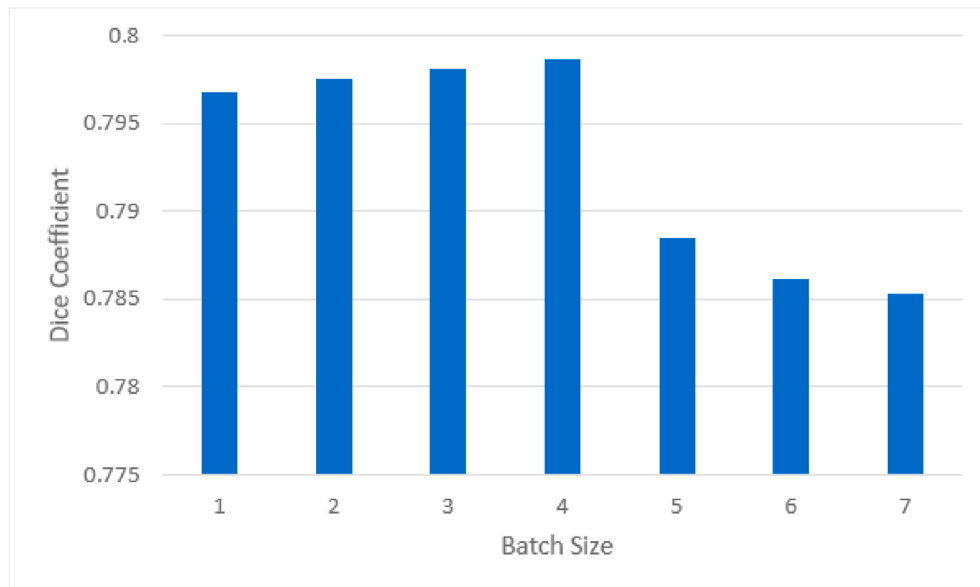


Fig. 7. The results of our method with different values of batch size.

Table 4

Average execution time for each method.

	Execution time (s)
Our method	0.39
Single U-Net	0.38
Attention U-Net	0.44
R2U-Net	0.47
R2AttU-Net	0.50

database. The experimental results show that our segmentation method outperforms these 20 methods.

In the future, we will investigate the performance of incorporating multiresolution and multiscale convolution filtering into Attention U-Net, R2U-Net and R2AttU-Net.

Declaration of competing interest

The authors declare that they have no conflict of interest.

Acknowledgement

Dr. Jiang conducted experiments and data analysis and drafted the manuscript. Dr. Ou helped to conduct experiments. Dr. Sen helped data analysis. Dr. Rehan provided a review and helped edit the manuscript. Dr. Yong provided a review and helped edit the manuscript.

Appendix A. Supplementary data

Supplementary data to this article can be found online at <https://doi.org/10.1016/j imu.2021.100602>.

References

- [1] Ichikawa M, Katahira K, Matsumoto Y, Seo K, Ochiai R, Kobayashi Y, Sakuma H. "Assessment of coronary artery disease using magnetic resonance coronary angiography: a national multicenter trial.". *J Am Coll Cardiol* 2010;56(12):983–91.
- [2] Hao D, Ding S, Qiu L, Lv Y, Fei B, Zhu Y, Qin B. "Sequential vessel segmentation via deep channel attention network.". *Neural Network* 2020;128:172–87.
- [3] Samuel PM, Veeramalai T. VSSC net: vessel specific skip chain convolutional network for blood vessel segmentation.". *Comput Methods Prog Biomed* 2021; 198.
- [4] Lee T, Kashyap R, Chu C. "Building skeleton models via 3-D medial surface Axis thinning algorithms.". *CVGIP Graph Models Image Process* 1994;56(Issue 6).
- [5] Szegedy C, et al. Going deeper with convolutions. Boston: IEEE Conference on Computer Vision and Pattern Recognition; 2015. p. 1–9.
- [6] Frangi F, Niessen J, Vincken L, Viergever M. "Multiscale vessel enhancement filtering," medical image computing and computer-assisted intervention. 1998.
- [7] Sato Y, Nakajima S, Shiraga N, Atsumi H, Yoshida S, Koller T, Kikinis R. Three-dimensional multi-scale line filter for segmentation and visualization of curvilinear structures. *Med Image Anal* 1998;2(2):143–68.
- [8] Wang S, Li B, Zhou S. "A segmentation method of coronary angiograms based on multi-scale filtering and region-growing.". International Conference on Biomedical Engineering and Biotechnology 2012:678–81.
- [9] Fazlali H, Karimi N, Soroushmeir S. "Vessel segmentation and catheter detection in X-ray angiograms using superpixels.". *Med Biol Eng Comput* 2018;56:1515–30.
- [10] Kass M, Witkin A, Terzopoulos D. Snakes: active contour models. *Int J Comput Vis* 1988;1:321–31.
- [11] Ifeoma N, Liana L. Fast temporal tracking and 3D reconstruction of a single coronary vessel. *IEEE International Conference on Image Processing* 2007:537–40.
- [12] Zhang D, Sun S, Wu Z, Chen B, Chen T. Vessel tree tracking in angiographic sequences. *J Med Imaging* 2017;4(2).
- [13] Zhou S, Yan J, Wang Y, Chen W. Automatic segmentation of coronary angiograms based on fuzzy inferring and probabilistic tracking. *Biomed Eng Online* 2010;9:40.
- [14] Melinscak M, Prentasic P, Lonaric S. "Retinal vessel segmentation using deep neural networks," proceeding of the 10th international conference on computer vision theory and applications. VISAPP; 2015.
- [15] Fu H, Xu Y, Lin S, Wong K, Liu J. 1DeepVessel: retinal vessel segmentation via deep learning and conditional random field. In medical image computing and computer-assisted intervention. 2016.
- [16] Cervantes-Sanchez F, Cruz-Aceves I, Hernandez-Aguirre A, Hernandez-Gonzalez M, Solorio-Meza S. Automatic segmentation of coronary arteries in X-ray angiograms using multiscale Analysis and artificial neural networks. *Appl Sci* 2019;9: 5507.
- [17] Nasr-Esfahani E, Samavi S, Karimi N, Soroushmeir S, Ward K, Jafari M, Felfeliyan B, Nallamothu B, Najarian K. Vessel extraction in X-ray angiograms using deep learning. *IEEE Engineering in Medicine and Biology Society Annual International Conference Aug.* 2016:643–6.
- [18] Yang S, Kweon J, Roh J. Deep learning segmentation of major vessels in X-ray coronary angiography. *Sci Rep* 2019;9:16897.
- [19] Tae Joon J, Jihoon K, Young-Hak Kim, Daeyoung K. "T-Net: nested encoder-decoder architecture for the main vessel segmentation in coronary angiography", *Neural Networks*. 2020.
- [20] Karel Z. "Contrast limited adaptive histogram equalization", *Graphics Gems IV*. Academic Press Professional, Inc.; 1994. p. 474–85.
- [21] Otsu N. A threshold selection method from gray-level histograms. *IEEE Transactions on Systems, Man, and Cybernetics Jan.* 1979;9(1):62–6.
- [22] Ridler T, Calvard S. Picture thresholding using an iterative selection method. *IEEE Transactions on Systems, Man, and Cybernetics Aug.* 1978;8(8):630–2.
- [23] Wayne N. An introduction to digital image processing. Strandberg Publishing Company; 1985.
- [24] Kittler J, Illingworth J, Foglein J. Threshold selection based on a simple image statistic. *Comput Vis Graph Image Process* 1985;30(2):125–47.
- [25] Long J, Shelhamer E, Darrell T. Fully convolutional networks for semantic segmentation. *arXiv*; 2015.
- [26] Alom MZ, Hasan M, Yakopcic C, Taha TM, Asari VK. Recurrent residual convolutional neural network based on U-net (R2U-net) for medical image segmentation. *arXiv*; 2018.
- [27] Wang Y, He Z, Xie P, Yang C, Zhang Y, Li F, Chen X, Lu K, Li T, Zhou J, Zuo K. "Segment medical image using U-net combining recurrent residuals and attention", *medical imaging and computer-aided diagnosis*. 2020. p. 77–86.
- [28] Pratt WK. Digital image processing. fourth ed. Los Altos, California: John Wiley and Sons, Inc.; 2007.
- [29] Li Y, Zhou S, Wu J, Ma X, Peng K. A novel method of vessel segmentation for X-ray coronary angiography images. *Fourth International Conference on Computational and Information Sciences*; 2012. p. 468–71.
- [30] Krizhevsky A, Sutskever I, Hinton G. ImageNet classification with deep convolutional neural networks. *Commun ACM* 2017;60(6):84–90.
- [31] Simonyan K, Zisserman A. Very deep convolutional networks for large-scale image recognition. *International Conference on Learning Representations*; 2015.
- [32] Sauvola J, Pietikäinen M. Adaptive document image binarization. *Pattern Recogn* 2000;33(2):225–36.
- [33] Szegedy C, Liu W, Jia Y, Sermanet P, Reed S, Anguelov D, Erhan D, Vanhoucke V, Rabinovich A. Going deeper with convolutions. *arXiv*; 2014.
- [34] Oktay O, Schlemper J, Folgoc L, Lee M, Heinrich M, Misawa K, Mori K, McDonagh S, Hammerla N, Kainz B, Glocker B, Rueckert D. Attention U-net: learning where to look for the pancreas. *arXiv*; 2018.
- [35] Kapur J, Sahoo P, Wong A. A new method for gray-level picture thresholding using the entropy of the histogram. *Comput Vis Graph Image Process* 1985;29(3): 273–85.
- [36] Hastie T, Tibshirani R, Friedman JH. The elements of statistical learning: data mining, inference, and prediction. New York: Springer; 2001.
- [37] Kang W, Kang W, Li Y, Wang Q. "The segmentation method of degree-based fusion algorithm for coronary angiograms," *International Conference on Measurement, Information and Control*; 2013. p. 696–9.
- [38] White J, Rohrer G. Image thresholding for optical character recognition and other applications requiring character image extraction. *IBM J Res Dev Jul.* 1983;27(4): 400–11.
- [39] A. Rosenfeld and P. De La Torre, "Histogram concavity analysis as an aid in threshold selection," In *IEEE transactions on systems, man, and cybernetics*, vol. SMC-13, no. 2, pp. 231–235, March-April 1983.
- [40] Najman L, Schmitt M. In: "Watershed of a continuous function," in signal processing (special issue on mathematical morphology), vol. 38; 1994. p. 99–112.
- [41] Nikhil R, Sankar K. Entropic thresholding. *Signal Process* 1989;16(2):97–108.
- [42] Ronneberger O, Fischer P, Brox T. "U-Net: convolutional networks for biomedical image segmentation". *Medical Image Computing and Computer-Assisted Intervention* 2015;9351:234–41.
- [43] Wan T, Shang X, Yang W, Chen J, Li D, Qin Z. Automated coronary artery tree segmentation in X-ray angiography using improved Hessian based enhancement and statistical region merging. *Comput Methods Progr Biomed* 2018;157.
- [45] Kerkeni A, Benabdallah A, Manzanares A, Bedoui M. A coronary artery segmentation method based on multiscale analysis and region growing. *Comput Med Imag Graph* 2016;48:49–61.
- [46] Zhu X, Cheng Z, Wang S, Chen X, Lu G. Coronary angiography image segmentation based on PSPNet. *Comput Methods Progr Biomed* 2021;200.
- [47] Ramponi G. A cubic unsharp masking technique for contrast enhancement. *Signal Process* 1998;67:211–22.
- [48] Frangi A, Niessen W, Vincken K, Viergever M. Multiscale vessel enhancement filtering. Medical image computing computer-assisted intervention. 1998.
- [49] Dice LR. Measures of the amount of ecological association between species. *Ecology* 1945;26(3):297–302.
- [50] Eiho S, Qian Y. Detection of coronary artery tree using morphological operator. *Comput Cardiol* 1997:525–8.
- [51] Tsai W. Moment-preserving thresholding: a new approach. *Comput Vis Graph Image Process* 1985;29(3):377–93.